Optical Engineering

OpticalEngineering.SPIEDigitalLibrary.org

Polarization beam splitter constructed by symmetrical metal-cladding waveguide

Hailang Dai
Jianfeng Shang
Xianfeng Chen

SPIE.

Hailang Dai, Jianfeng Shang, Xianfeng Chen, "Polarization beam splitter constructed by symmetrical metal-cladding waveguide," *Opt. Eng.* **56**(7), 077107 (2017), doi: 10.1117/1.OE.56.7.077107.

Polarization beam splitter constructed by symmetrical metal-cladding waveguide

Hailang Dai,[a,b] Jianfeng Shang,[a,b] and Xianfeng Chen[a,b,*]
[a]Shanghai Jiao Tong University, State Key Laboratory of Advanced Optical Communication Systems and Networks, Department of Physics and Astronomy, Shanghai, China
[b]Shanghai Jiao Tong University, Collaborative Innovation Center of IFSA (CICIFSA), Shanghai, China

Abstract. A structure of polarization beam splitter based on a symmetrical metal-cladding waveguide (SMCW) was demonstrated. The light beam energy can be coupled into the SMCW directly through free space without additional coupler. By introducing anisotropic material into the guided layer, different excitation conditions for transverse-electric and transverse-magnetic modes are obtained, which results in polarization-dependent reflection. The propagation loss that is mainly caused by the metal absorption is <2 dB. [DOI: 10.1117/1.OE.56.7.077107]

Keywords: beam splitter; polarization-selective devices; waveguide.

Paper 170612 received Apr. 24, 2017; accepted for publication Jun. 27, 2017; published online Jul. 19, 2017.

1 Introduction

Polarization beam splitter (PBS) is a basic optical element that can separate a light beam into two orthogonally polarized beams. It has been widely used in optical systems, such as magneto-optical data storage, free-space optical switching, image processing, and so on. In addition to the conventional PBS, which relies on the inherent birefringence of anisotropic materials, various other methods for PBS and principles and structures have been proposed during the past few years, such as binary blazed grating coupler,[1] embedded metal-wire nanograting,[2,3] anisotropic metamaterial slab,[4,5] and coupled plasmonic waveguide arrays.[6] Several types of PBS based on photonic crystals have also been reported,[7–11] which are based on the facts that the bandgaps for transverse-electric (TE) and transverse-magnetic (TM) polarization occur at different wavelength ranges and the polarization-dependent dispersion properties of such photonic crystals. Each kind of structure, however, has a fixed and relatively narrow wavelength range. Hence, finding a new device to circumvent these limitations has become an urgent issue.

Over the past decades, the symmetrical metal-cladding waveguide (SMCW), which sustains the ultrahigh-order-guided modes, has been intensively investigated. Ultrahigh-order-guided modes in SMCW possess many fascinating characteristics, such as small propagation constant, strong modes density, and large Goos–Hänchen shift.[12] Various applications based on the SMCW have been proposed, such as slow light,[13,14] superprism spectrometers,[15] and precise displacement detection.[16,17] The free-space light beam can be transferred into SMCW from the top metal surface directly.[18] For a high-quality factor sample, most of the light energy can be coupled into the waveguide.

In this paper, we experimentally demonstrated a new device to realize the same function of PBS based on a peculiar structure of SMCW. A single crystalline lithium niobate (LN) slab was used as the guided layer. Owing to the anisotropic property of the LN crystal, the TE and TM modes have different resonance angles. When the incident angle of the light meets the resonance angle, the high transmission is obtained for one polarization, and the other polarization will be largely reflected. Whilst the coupling layer of SMCW radiative damping related to the permittivity of metal which has been relationship with the incident light frequency. So that radiative losses of SMCW are changed by the different of incident light frequency. In SMCW, the thickness of coupling layer can be designed by thermal evaporation. We can design a performance thickness to achieve a highly effectively coupled [18] to an incident light frequency, due to the coupled effective of incident light is strongly dependent on the thickness of the top silver film. This kind of PBS is suitable for a large wavelength range by designed kinds of thickness, which make it more applicative in optical information reflection.

2 Method and Waveguide Structure

Compared with the conventional all-dielectric optical waveguides, a thick SMCW possesses lots of fascinating optical properties. The most important feature is the existence of ultrahigh-order-guided modes. The order of guided modes in a sub-mm SMCW can be much higher than 1000. Thus, the polarization-dependent phase shift in total internal reflection at the dielectric/metal interface can be negligible.[12] For an optical waveguide consisting of a thick guided layer and two metal-cladding layers, the reduced dispersion equation for ultrahigh-order modes can be written as

$$k_0 h\sqrt{n^2 - N^2} = m\pi, \tag{1}$$

where $k_0 = 2\pi/\lambda$ is the propagation constant in vacuum, h and n are the thickness and the refractive index of the guided layer, respectively. $N = \beta/k_0$ is the effective refractive index, where β is the propagation constant of guided modes,

*Address all correspondence to: Xianfeng Chen, E-mail: xfchen@sjtu.edu.cn

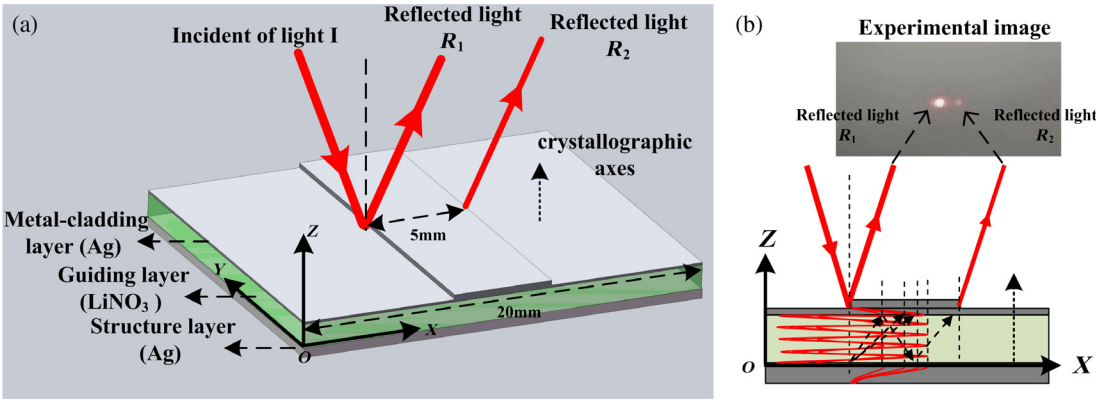

Fig. 1 (a) Schematic diagram of the SMCW, which contains three layers and a sliver stripe. (b) Principle of the incident light beam transmission and reflection.

and m is the modes order. Expect for the high modes order, another characteristic of ultrahigh-order modes in SMCW is that the effective refractive index is extremely small, which usually less than the refractive index of air.

In our experiment, the schematic diagram of the SMCW is shown in Fig. 1(a). A 0.5-mm thick of LN crystal is used as guided layer, and a thin silver film (about 40-nm thick) of upper layer is used to couple the pump light into the waveguide. Another 300-nm thick silver film serves as the substrate layer. In the middle part of the couple layer, an additional thick (about 150-nm thick and 5-mm width) silver stripe was fabricated to prevent light leakage. As shown in Fig. 1(b), the left and right parts of the silver stripe are used to excite and couple out the ultrahigh-order modes, the light beam R_1 is reflected by the metal-cladding layer and the light beam R_2 is "reflected" after passing through the silver stripe. According to the phase-matching principle, the out-coupling angle of beam R_2 is the same as in-coupling angle, therefore reflected beams R_1 and R_2 are in parallel with each other.

From Eq. (1), it is obvious that the SMCW is polarization degenerated for an isotropic-guided medium. While for an anisotropic-guided layer, SMCW becomes polarization-dependent due to birefringence of the guided medium. The optical axis of LN is along z direction, which means that the SMCW in our experiment is a polarization-sensitive device for the incident beam. When a light beam incidents onto the coupling surface of the SMCW, an ultrahigh-order mode will be excited under the phase-matching condition. As shown in Fig. 2, we calculated the reflectivity spectral of the ultrahigh-order modes for both TE and TM polarization beams in the conditions of $\lambda = 680$ nm, $h = 0.5$ mm, and the thickness of the metal-cladding layer is near to 40 nm. And Fig. 2 plots a calculated reflectivity of the SCMW, which can be excited by the free spacing coupling technology,[16] since the effective index of the SCMW is less than unit. When the phase-matching condition is fulfilled, energy is transferred from the reflected light and coupled into the guided layer; thus, a reflection dip is formed in the reflection spectrum near the resonance angle, and the optical intensity in the guided layer is greatly enhanced compared with the incident light. The calculated reflectivity is simulated in ATR V2.03 software by us. And the parameters of simulation are the same as the experimental sample. The dielectric constant of $LiNbO_3$ and the silver are $\varepsilon_0 = 5.27$, $\varepsilon_e = 4.88$, and $\varepsilon_{Ag} = -22.14 + i0.51$. The reflectivity for each polarization

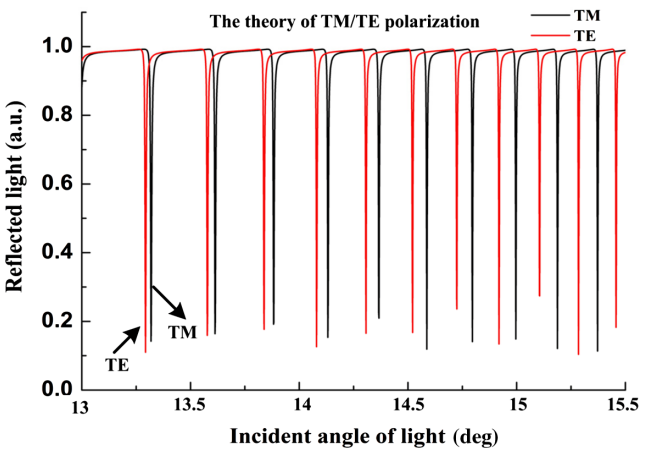

Fig. 2 Calculated reflectivity spectrum of the TE and TM modes with respect to the incident angle.

strongly varies with the incident angle in the range of a guided mode. We can also see that the coupling angles of TE and TM modes are staggered from each other, which give rise to different reflections and transmissions of such different polarized modes. When the incident angle match with mode resonance angle of TE polarization, the beam energy of TE polarization will be efficiently coupled into the waveguide and will be coupled out on the opposite side of the silver stripper. At this condition, completely different with TE polarization, the beam energy of TM polarization will be thoroughly reflected.

3 Experiment and Results

The schematic diagram of the experimental setup was shown in Fig. 3. In the experiment, a solid-state laser (680 nm, 25 mW diode-pumped solid-state laser, Shanghai Optical Engine Inc., Shanghai, China) was used. Two apertures with diameters of 1 mm were inserted to confine the divergence of the incident light. The polarizer was used to transform the linear polarized light beam into the elliptical polarized laser beam. Then, the incident beam passed through a hole on the optical screen and incident on the thin silver film of the SMCW. The SMCW was vertically located on a computer controlled $\theta/2\theta$ goniometer that could adjust the incident angle precisely. Finally, the ultrahigh-order modes of

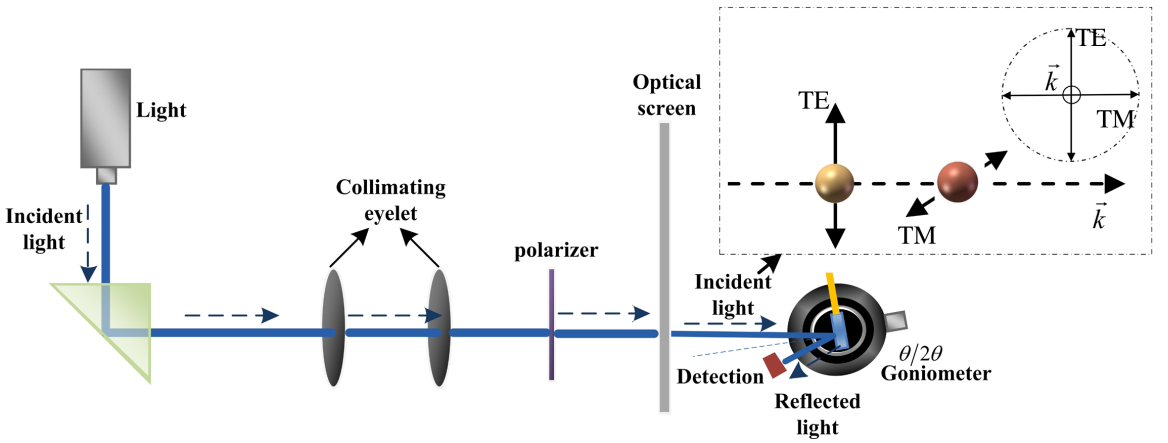

Fig. 3 Configuration of the experimental setup.

the SMCW could be excited, and the reflected light was tested by a polarization analyzer.

The experimental transmission spectra of TE and TM polarization beams were measured and shown in Fig. 4(a). The incident angle of the pump light ranged from 14.2 deg to 15.45 deg, which was precisely adjusted by utilizing a rotation stage. When the angle satisfies the mode coupling condition, the reflected light intensity of the light could be measured by a photodetector. We could clearly see that the intensity picks of the TE and TM modes were separated with each other, which means that the waveguide could only transmit TE or TM modes in the fixed incident angle. Then, the reflected light spectra of elliptical polarization beam were also measured as shown in Fig. 4(b). The intensity picks were in good agreements with the picks that show in Fig. 4(a). The reflected light picks of TE and TM modes appear alternately with the incident angle changing.

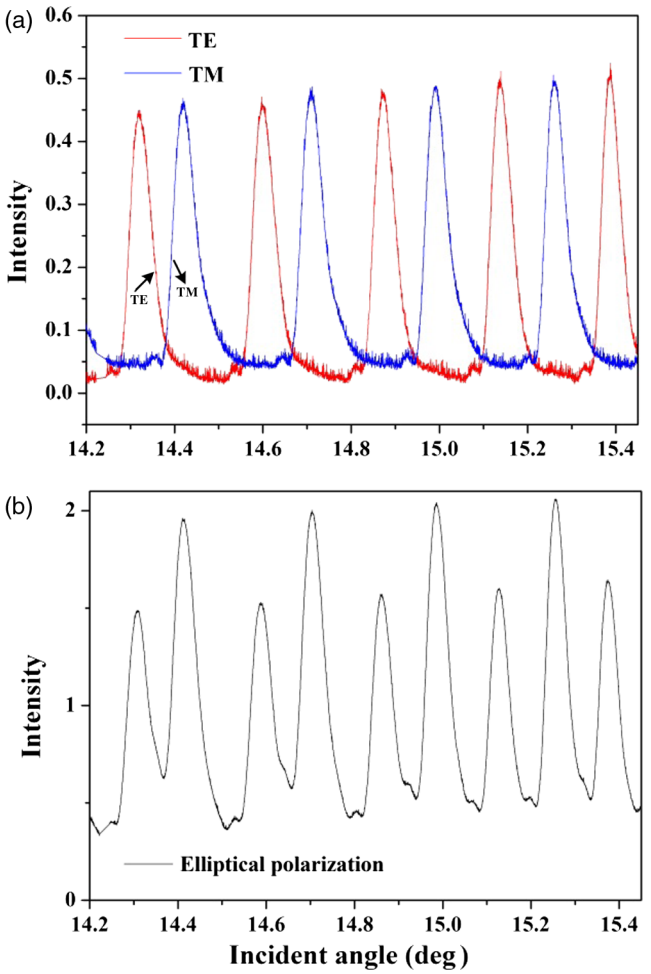

Fig. 4 (a) The experimental reflected light spectra of both TE and TM polarization beams at the wavelength of 680 nm. (b) The experimental reflected light spectra of elliptical polarization beam at the wavelength of 680 nm.

4 Discussion

The coupling efficiency μ of the light beam is mainly determined by the thickness of the metal-cladding layer (silver was used in our experiment). According to electromagnetic field boundary conditions, the coupling efficiency μ can be expressed as

$$\mu = \frac{4\,\mathrm{Im}(\beta^0)\mathrm{Im}(\Delta\beta^L)}{[\mathrm{Im}(\beta^0) + \mathrm{Im}(\Delta\beta^L)]^2}, \tag{2}$$

where $\mathrm{Im}(\beta^0)$ and $\mathrm{Im}(\Delta\beta^L)$ are intrinsic and radiative damping, respectively. When $\mathrm{Im}(\beta^0) = \mathrm{Im}(\Delta\beta^L)$, the coupling efficiency $\mu = 1$ and it also represents the matching condition coupling incident angles θ for the excitation of the guided modes due to $\mathrm{Im}(\beta^0)$ and $\mathrm{Im}(\Delta\beta^L)$ are determined by the dielectric constant of metal and incident angle.[17] In this paper, we consider the coupling efficiency $\mu = 1 - R$. The R is reflective of light.

In order to reduce the reflective efficiency, we calculate the coupling efficiency of both TE- and TM-polarized light beams at the wavelength of $\lambda = 680$ nm. We set the incident angles at the coupling angle for the TE mode ($\theta_1 = 14.10$ deg) and the TM mode ($\theta_2 = 15.20$ deg), respectively. As shown in Fig. 5, the coupling efficiency is observably altered with the thickness of metal-cladding layer. When the thickness of the metal-cladding layer reaches to 40 nm the coupling efficiency obtains the maximum value. The coupling efficiency will dramatically decrease, for the thickness of the coupling layer is too thick or too thin. In the experiment, when the thickness of the metal-cladding

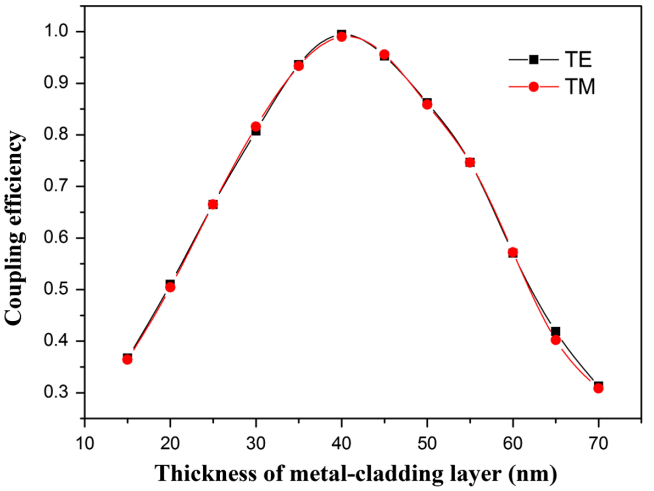

Fig. 5 Calculated coupling efficiency of TE and TM polarization with respect to the thickness of the metal-cladding layer.

layer near to 40 nm, the coupling efficiency of both TE and TM polarization approach to 90%.

The metal absorption in optical frequency would be an unavoidable problem; in fact, the loss could be greatly reduced by extending the thickness of guided layer to sub-mm or mm scale.[14] In our experiment, the thickness of the guided layer is 0.5 mm and the propagation loss is <2 dB.

5 Conclusion

In summary, a novel structure of SMCW to achieve splitting of TE and TM polarizations of the light beam was proposed. Owing to the birefringence effect of the anisotropy material using in the guided layer, polarization-dependent reflected light could be obtained in such SMCW structure. When the incident angle met with the resonance angle, large reflected light of TE (TM) polarization was obtained, on the contrary, TM (TE) polarization was highly reflected. Using SMCW PBS, it is applicative for a wide wavelength range and gets rid of the limitation of Brewster angle. Besides, the additional coupler was not needed in this structure, which makes it flexible in design and application.

Acknowledgments

This work was supported in part by the National Natural Science Foundation of China (NSFC) under Grant No. 61235009 and the National Basic Research Program of China under Grant No. 2013CBA01703.

References

1. J. Feng and Z. Zhou, "Polarization beam splitter using a binary blazed grating coupler," *Opt. Lett.* **32**, 1662–1664 (2007).
2. L. Zhang et al., "Design and fabrication of metal-wire nanograting used as polarizing beam splitter in optical telecommunication," *J. Optoelectron. Adv. Mater.* **8**, 847–850 (2006).
3. L. Zhou and W. Liu, "Broadband polarizing beam splitter with an embedded metal-wire nanograting," *Opt. Lett.* **30**, 1434–1436 (2005).
4. H. Luo, Z. Ren, and W. Shu, "Construct a polarizing beam splitter by an anisotropic metamaterial slab," *Appl. Phys. B* **87**, 283–287 (2007).
5. J. Zhao, Y. Chen, and Y. Feng, "Polarization beam splitting through an anisotropic metamaterial slab realized by a layered metal-dielectric structure," *Appl. Phys. Lett.* **92**, 071114 (2008).
6. C. Y. Tai, S. H. Chang, and T. C. Chiu, "Design and analysis of an ultra-compact and ultra-wideband polarization beam splitter based on coupled plasmonic waveguide arrays," *IEEE Photonics Technol. Lett.* **19**, 1448–1450 (2007).
7. X. Ao and S. He, "Polarization beam splitters based on a two-dimensional photonic crystal of negative refraction," *Opt. Lett.* **30**, 2152–2154 (2005).
8. Z. Lu, Y. Tang, and Y. Shen, "Polarization beam splitting in two-dimensional photonic crystals based on negative refraction," *Phys. Lett. A* **346**, 243–247 (2005).
9. V. Mocella, P. Dardano, and L. Moretti, "A polarizing beam splitter using negative refraction of photonic crystals," *Opt. Express* **13**, 7699–7707 (2005).
10. S. Kim, G. P. Nordin, and J. Cai, "Ultracompact high-efficiency polarizing beam splitter with a hybrid photonic crystal and conventional waveguide structure," *Opt. Lett.* **28**, 2384–2386 (2003).
11. A. M. Vyunishev and A. S. Chirkin, "Multiple quasi-phase-matching in nonlinear Raman-Nath diffraction," *Opt. Lett.* **40**(2), 1314–1317 (2015).
12. H. Lu, Z. Cao, and H. Li, "Study of ultrahigh-order modes in a symmetrical metal-cladding optical waveguide," *Appl. Phys. Lett.* **85**, 4579–4581 (2004).
13. W. Yuan et al., "Wideband slow light assisted by ultrahigh-order modes," *J. Opt. Soc. Am. B* **28**, 968–971 (2011).
14. Y. Zheng, W. Yuan, and X. Chen, "Wideband slow-light modes for time delay of ultrashort pulses in symmetrical metal-cladding optical waveguide," *Opt. Express* **20**, 9409–9414 (2012).
15. Y. Wang, Z. Cao, and T. Yu, "Enhancement of the superprism effect based on the strong dispersion effect of ultrahigh-order modes," *Opt. Lett.* **33**, 1276–1278 (2008).
16. F. Chen, Z. Cao, and Q. Shen, "Picometer displacement sensing using the ultrahigh-order modes in a submillimeter scale optical waveguide," *Opt. Express* **13**, 10061–10065 (2005).
17. L. Chen, Z. Cao, and F. Ou, "Observation of large positive and negative lateral shifts of a reflected beam from symmetrical metal-cladding waveguides," *Opt. Lett.* **32**, 1432–1434 (2007).
18. H. Li, Z. Cao, and H. Lu, "Free-space coupling of a light beam into a symmetrical metal-cladding optical waveguide," *Appl. Phys. Lett.* **83**, 2757–2759 (2003).

Hailang Dai a physical doctor student level 2016 in Shanghai Jiaotong University (SJTU), Shanghai, China and Professor Chen Xianfeng is his supervisor. He is also with the State Key Laboratory of Advanced Optical Communication System and Networks, SJTU. His research field is optoelectronic devices.

Biographies for the other authors are not available.